Investigation of Induction Heating for Sheet Metal with Moving Induction Coil

Raphael Gergely* and Christoph Hochenauer
Institute of Thermal Engineering, Graz University of Technology, 8010 Graz, Austria
Email: raphael.gergely@tugraz.at (R.G.), christoph.hochenauer@tugraz.at (C.H.)

***Abstract*—The efficiency of induction heating is highly dependent on the coil geometry and the air gap between the coil and the workpiece, therefore the aim of this research is to experimentally evaluate the efficiency and uniformity of temperature distribution in induction heating, utilizing an inductor coil, movable in three axes. The experiment is conducted under the condition that the inductor coil is not tailored for the specific workpiece, giving it a higher flexibility compared to the conventional application of induction heating. To achieve this objective, a downscaled test bench was designed, employing a CNC machine for execution. In addition, in this study, a second test bench was built to establish an analytical approach in determining the parameter field between power, air gap and efficiency. The steady-state conditions in this test bench allowed the closure of the energy balances to be calculated analytically, allowing immediate validation of the accuracy of the results. This parameter field was utilized to evaluate the outcomes of the moving inductor experiments.**

***Index Terms*—Efficiency, induction heating, moving coil, steady state**

I. Introduction

Induction heating finds widespread utility across various industrial applications [1, 2]. An important advantage of induction heating is its superior efficiency relative to other methods of heating [1]. Induction generates the heat directly in the workpiece without relying on other transfer methods like radiation convection or conduction. The power transfer density can reach up to 30,000 W/cm^3 [2]. High efficiency is particularly crucial in the era of global warming and the global need to decrease CO_2 emissions.

One drawback of induction heating is that the eddy currents that cause the heating are highly concentrated, resulting in heating of the material within a limited area beneath the induction coil. The effects which lead to the distribution of the eddy currents are well documented in literature and the most important are:

- Skin effect [2–5]
- Proximity effect [6]
- Slot effect [6]
- End and edge effect [7]

A small air gap between the induction coil and the workpiece is necessary for an efficient application of the heating process. Therefore, in many cases, the induction coil is designed specifically for a single application. For example, when sheet metal is heated using induction heating, the induction coil is typically the same width as the workpiece which continuously moves under the fixed coil, as described by Vibrans [8] for sheet metal and by Liu *et al*. [9] for welded pipes. Sun *et al*. [10] investigated the continuously heating of inner corrugated section experimentally and numerically for different geometries of the inductor and air gaps. This method has demonstrated its efficiency but lacks flexibility. It would not be practical to switch the coil between every workpiece if induction heating is used for a more adaptable production line. Similarly, if the width of the workpieces is too wide, using an induction coil of equal width would not be viable.

This work suggests a setup featuring a smaller induction coil capable of moving in three axes over the workpiece. This concept was tested at a reduced scale. The setup allows for the use of a narrower induction coil compared to the workpiece's width. Two crucial parameters were utilized to assess the effectiveness of the demonstrated heating strategy: Efficient initial heating and uniform temperature distribution (to prevent issues such as thermal stresses).

Assessing the efficiency of induction heating is challenging due to the complex nature of the magnetic and hence temperature fields. As such, previous works [10–13] have mainly focused on numerical investigations of the subject. Another topic that many previous works have focused on has been the investigation of the uniformity of the temperature field with respect to geometry optimisation. Patil *et al*. [14] numerically studied the temperature field of steel bars and Jin *et al*. [15] studied the distribution in a plate with respect to the geometry of a static inductor. Other numerical simulations dealing with the heating of tubes include Fu *et al*. [16] for sodium-filled tubes and Wen *et al*. and Wang *et al*. [17] for inner linings of tubes, focusing on the uniformity of the temperature field. The influence of magnetic flux concentrators (MFCs) on the induction heating process has been shown by Wen *et al*. [19] for the hardening of gears and by Yang *et al*. [20] where adjustable MFCs were discussed.

Most of the above-mentioned works investigated induction heating numerically or compared a numerical simulation with experiments. The focus of this paper is to present an experimental setup that allows for the analytical investigation of the efficiency of a coil, and then to

Manuscript received November 23, 2023; revised January 12, 2024; accepted January 28, 2024.
*Corresponding author.

compare the calculated parameter field with an experiment that more closely reflects an industrial application to prove the usefulness of the parameter field. Therefore, the first step in this study was to pre-measure the induction coil in steady state conditions, which allowed a simple calculation of a parameter field for power, air gap and efficiency of the inductive heating device without the need to know the exact geometry of the magnetic field and therefore the temperature field. This was done analytically using equations derived from thermodynamics. Another notable advantage of this method is the ability to analytically check the closure of the energy balances for the entire system, allowing immediate validation of the measurements. These steady-state experiments were then used in this work to later evaluate the efficiency of the transient sheet metal experiments, serving as an upper limit of efficiency and validation for the experiment's results, instead of the numerical investigation shown in the literature above.

II. Steady-State Experiments for Determining The Parameter Field for Comparison

The objective of this series of experiments was to determine the correlation between the electric power of the inductor, the air gap, and efficiency. A similar setup (tube with inductor on one side) has been numerically investigated by Zhang *et al*. [18] also for different air gaps and inductor output powers for molten salt in receiver tubes. The experimental setup enabled steady-state measurements, which allowed for analytical efficiency calculations, thus eliminating the need for numerical considerations.

The following parameters were varied during the experiments:

- Power of the inductor (DC)
- Air gap between inductor and the workpiece
- Material of the heated pipe
  - ✓ Unalloyed steel
  - ✓ Stainless steel

The following parameters were measured:

- In- and outlet temperature of the test rig and the inductor
- Mass flow of water through the test bench
- Mass flow of cooling water through the inductor
- Surface temperature of the heated pipe
- Drawn electrical power of the induction heating device

The experimental setup is depicted in Fig. 1 and Fig. 2, where a schematic and a picture of the test rig are provided. Water flows into the rig via the inlet (1) and mass flow is measured using a magnetic inductive flow meter (3) positioned further downstream. Temperature sensors (4, 9) are used to measure inlet and outlet temperatures. An induction coil (5) is used to heat the 1-inch pipe, which can be exchanged between unalloyed and stainless steel, in order to obtain parameter fields for both materials. The induction heating device is commercially available and can operate between 0.5 kW and 10.2 kW. A vortex generator (7) has been installed to increase the mixing of the laminar flow's distinct layers in the pipe and thus, achieve the mixed temperature of the flow after the inductor's heating.

In order to obtain all leading terms of the energy, measurements were conducted on the mass flow rate, inlet temperature, and outlet temperature of the cooling water flowing through the inductor, in addition to the inlet and outlet streams in the test rig. The inductor utilized in the experiments was a surface inductor with a single wound coil and additional magnetic flux concentrators with a width of 74 mm.

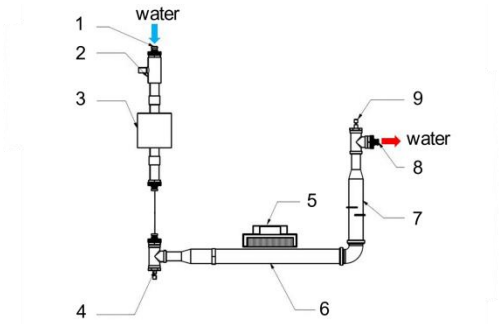

1 inlet
2 ball valve
3 mass flow meter
4 PT100 inlet temp. sensor
5 inductor coil
6 stainless steel/ unalloyed steel pipe
7 vortex generator
8 outlet
9 PT100 temp. sensor

Fig. 1. Schematic drawing of steady-state test bench.

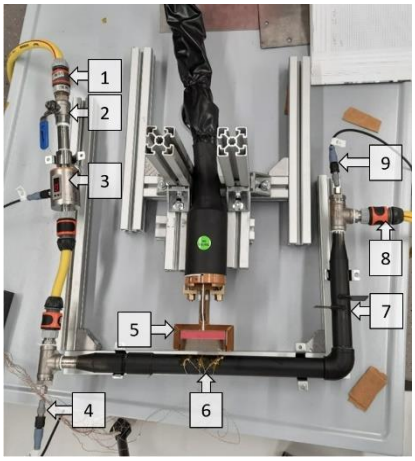

Fig. 2. Picture of steady-state test bench.

A. Execution of Steady-State Experiments

The aim of the test bench, as stated in the introduction, is to measure parameters while maintaining steady-state conditions. This data will help to provide a benchmark for subsequent validation of the transient experiments. It will also ensure their validity. In order to ensure steady-state conditions during the measurements, the temperature was recorded every second. The values for further calculations were derived after the outlet temperature and surface temperature of the heated pipe had reached steady-state conditions through measurements made using thermocouples and thermography. After steady-state conditions were achieved, all the aforementioned parameters were monitored for a duration of 100 s, and subsequently the mean for this time period was calculated.

The losses resulting from natural convection and radiation are assumed to be negligible. To obtain the temperature data of the pipe which was heated for experiment U3-2, a thermal imaging camera was used,

which revealed an average temperature in the near-field of the inductor of 63.7 ℃. Assuming an ambient temperature of 20 ℃ and a heat transfer coefficient of 10 W/(m ³K), it was calculated that the heat loss through natural convection amounts to 9.25 W. The radiant heat losses, with an emissivity of 0.85, was calculated to be 13.4 W. Both can be disregarded in comparison to the effective heat flow of the 4.65 kW induction heating device.

B. Calculations of Efficiency

The energy balances were calculated for different operating points using the given equations. The effective heat flux could be expressed as:

$$\dot{Q}_{\text{heat effective}} = \dot{m}_{\text{water}}\ \text{cp}_{\text{w}}\left(T_{\text{out rig}} - T_{\text{in rig}}\right), \qquad (1)$$

where the mass flow of water through the test bench $\dot{m}_{\text{water}}$ is multiplied by the specific heat capacity of water cp_{w} (4.19 kJ/(kg K)) [19], and the temperature difference between the inlet $T_{\text{in rig}}$ and the outlet $T_{\text{out rig}}$. Please note that temperatures used to determine the temperature difference are obtained during the steady-state phase of the experiment.

The device's heat loss is calculated using the same approach as the effective power and can be expressed as as follows:

$$\dot{Q}_{\text{heat loss}} = \dot{m}_{\text{cooling water}}\ \text{cp}_{w}(T_{\text{out ind}} - T_{\text{in ind}}) \qquad (2)$$

With the mass flow of the cooling water $\dot{m}_{\text{cooling water}}$ and the temperature difference of the cooling water ($T_{\text{out ind}}$ and $T_{\text{in ind}}$). The error in the energy balances is calculated by:

$$\text{Error} = \frac{P_{\text{DC}} - (\dot{Q}_{\text{heat effective}} + \dot{Q}_{\text{heat loss}})}{P_{\text{DC}}} \times 100\% \qquad (3)$$

Specifically, this equation computes the relative difference between the electrical power of the inductive heating device after the rectifier P_{DC}, and the sum of the effective power $\dot{Q}_{\text{heat effective}}$ and the cooling power $\dot{Q}_{\text{heat loss}}$ calculated beforehand.

The efficiency of the operation points can be calculated by:

$$\eta = \frac{\dot{Q}_{\text{heat effective}}}{P_{\text{el AC}}} \qquad (4)$$

Using the calculated effective heat flow of the inductor $\dot{Q}_{\text{heat effective}}$ and the electrical power consumed by the inductor $P_{\text{el AC}}$.

III. Planar Heating Experiments

The adopted planar heating strategy was intended to efficiently heat the sheet metal while maintaining an even surface temperature distribution. To achieve this, the inductor head was mounted to a small CNC milling machine, as shown in Fig. 3.

Four test series were carried out for the planar heating experiment, testing two sizes of workpieces (2× and 3× the width of the induction coil) and two materials (unalloyed and stainless-steel) to see if there is a decrease of efficiency if the workpiece width is increased. The workpieces and the path of the inductor coil are depicted in Fig. 4 and Fig. 5.

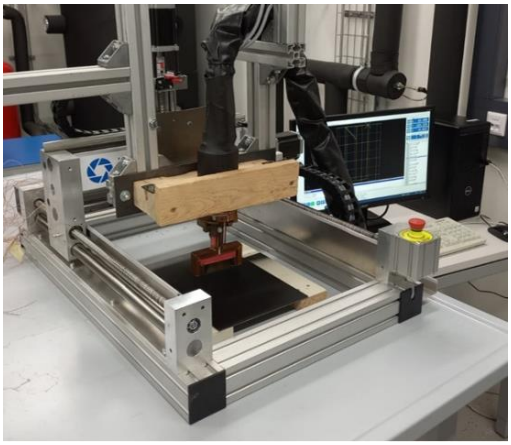

Fig. 3. Test bench of transient experiments.

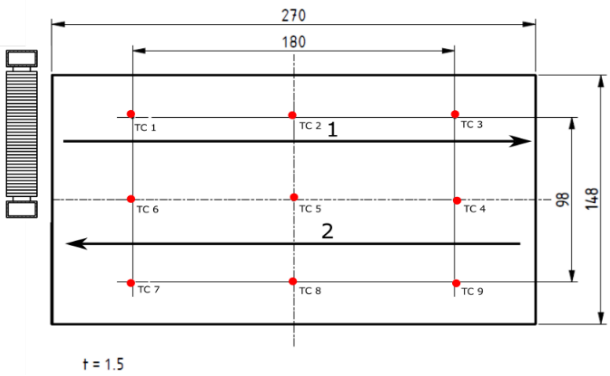

Fig. 4. Schematic of the smaller workpiece

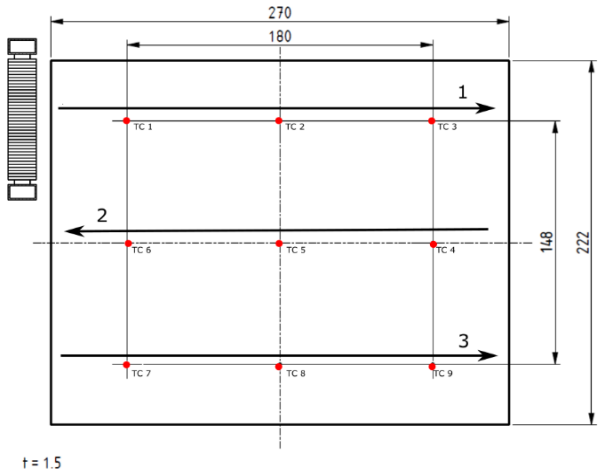

Fig. 5. Schematic of the larger workpiece.

The planar heating process involved positioning the induction coil at the edge of the part for the first pass and then moving along the length of the part, as visually indicated by the arrow marked '1'. Once the coil has traversed the entire workpiece, the power to the induction coil is switched off and the coil is moved across the width of the workpiece before being passed over again as shown by arrow '2'. This sequence is repeated for a third time (arrow '3'). For the smaller workpiece it was only

necessary to pass the workpiece 2 times to cover the whole surface area as indicated in Fig. 4.

The experiment was conducted using three air gaps ranging from 3 mm to 9 mm. With larger air gaps, the power was increased to maintain an approximate temperature of 140 ℃. The feeding speed of the CNC machine remained constant for all experimental series at a rate of 1500 mm/min for each longitudinal pass. Temperatures were monitored using nine thermocouples positioned under the workpiece, as displayed in Fig. 4 and Fig. 5 (TC 1–9).

Another experiment was conducted with the same setup to maintain the temperature at the level of initial heating for some time. Fig. 6 provides an example of this experiment. In this case, the inductor's power was reduced after it passed over the entire workpiece for the first time. The inductor coil subsequently moved over the workpiece with reduced power to maintain the temperature.

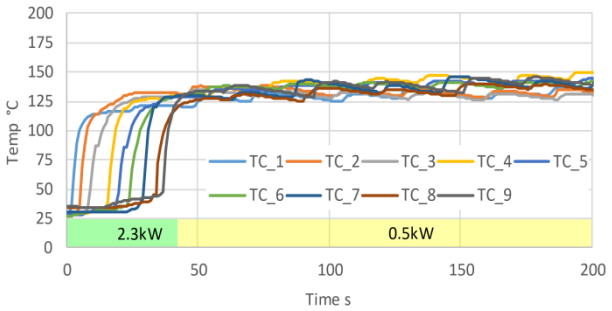

Fig. 6. Heating up and holding temperature.

A. Calculation of Efficiency for Transient Experiments

The inductor's effective power is determined by:

$$\dot{Q}_{\text{heat effective trans}} = \frac{m\ \text{cp}\ (T_{\text{ave.end}} - T_{\text{ave.start}})}{t_{\text{ind}}} \quad (5)$$

The workpiece's mass is represented by m and its specific heat capacity is cp (502 J/(kgK) for stainless steel and 490 J/(kg K) for unalloyed steel. The temperature at the beginning of the experiment is identified as $T_{\text{ave.start}}$, which is the average of the nine thermocouples used. The average end temperature ($T_{\text{ave.end}}$) was determined by averaging the temperature measurements from all 9 thermocouples after the initial heat up of the workpiece (when the inductor coil has passed the whole workpiece for the first time). t_{ind} represents the time at which the inductor was activated over the workpiece.

The overall efficiency of the transient experiments is calculated as follows:

$$\eta = \frac{\dot{Q}_{\text{heat effective trans}}}{P_{\text{el AC}}}\ , \quad (6)$$

by dividing the previously calculated effective power $\dot{Q}_{\text{heat effective trans}}$ by the electrical power consumed by the device $P_{\text{el AC}}$. Thus, the same calculation method used for the transient experiments was implemented to ensure comparability between the two experiments.

IV. Results of Experiments

A. Results of Steady-State Experiment

The findings from the steady-state experiments are presented in Fig. 7 for stainless steel and Fig. 8 for unalloyed steel, and additionally in Table I and Table II in more detail.

TABLE I: RESULTS STEADY-STATE EXPERIMENTS STAINLESS

Unit	Air gap mm	$P_{\text{el AC}}$ kW	$\dot{Q}_{\text{heat effective}}$ kW	$\dot{Q}_{\text{heat loss}}$ kW	η %	Error energy bal.%
S1-1	1	10.42	5.27	4.63	50.6	2.0
S1-2	1	6.2	3.05	2.93	49.2	−1.4
S1-3	1	3.06	1.37	1.57	44.7	−1.4
S1-4	1	1.05	0.34	0.60	31.9	−3.5
S3-1	3	10.56	4.64	5.38	43.9	2.7
S3-2	3	8.33	3.4	4.66	40.8	1.8
S3-3	3	5.11	2.01	2.76	39.4	0.5
S3-4	3	2.6	0.89	1.48	34.3	−3.3
S6-1	6	10.45	3.08	6.86	29.5	1.6
S6-2	6	6.94	2.01	4.56	29.0	−1.1
S6-3	6	4.24	1.11	2.84	26.2	1.3
S9-1	9	10.57	1.87	7.9	17.6	3.9
S9-2	9	8.85	1.62	6.84	18.3	0.5
S9-3	9	5.9	0.96	4.43	16.3	3.7

TABLE II: RESULTS STEADY-STATE EXPERIMENTS UNALLOYED

Unit	Air gap mm	$P_{\text{el AC}}$ kW	$\dot{Q}_{\text{heat effective}}$ kW	$\dot{Q}_{\text{heat loss}}$ kW	η %	Error energy bal.%
U1-1	1	10.56	7.32	2.81	69.3	0.8
U1-2	1	5.44	3.6	1.66	66.2	0.7
U1-3	1	3.54	2.12	1.2	59.9	2.3
U1-4	1	10.56	6.36	3.86	60.3	−0.2
U3-1	3	7.95	4.65	2.98	58.4	−1.7
U3-2	3	3.9	2.11	1.54	54.0	−1.4
U3-3	3	1.3	0.57	0.54	44.0	−1.2
U3-4	3	10.53	4.35	5.61	41.3	2.4
U6-1	6	8.4	3.41	4.65	40.6	0.6
U6-2	6	5.12	1.97	2.8	38.4	0.7
U6-3	6	2.57	0.93	1.5	36.2	−1.2
U9-1	9	10.53	2.98	6.99	28.3	2.3
U9-2	9	10.2	2.99	6.81	29.3	1.0
U9-3	9	6.9	1.89	4.56	27.3	2.3

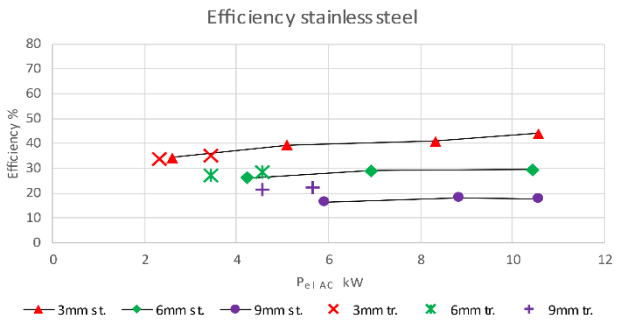

Fig. 7. Comparison steady-state(st.)/transient(tr.) for stainless steel.

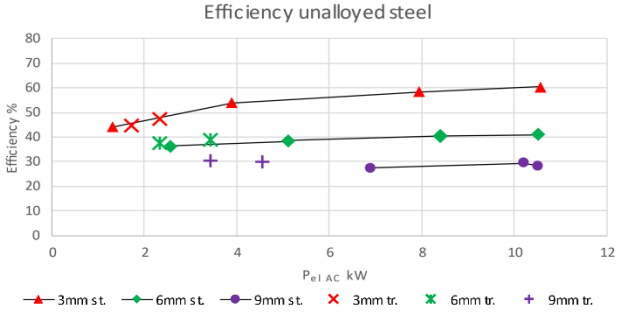

Fig. 8. Comparison steady-state(st.)/transient(tr.) for unalloyed steel.

Fig. 7 and Fig. 8 illustrate different air gaps, marked by colour, utilized in the experiments, with each air gap category varying the power of the inductor. To maintain the same conditions for each experimental series, the upper limit of the power was selected to prevent the boiling of water near the wall of the pipe. Lower-power experiments were not conducted for larger air gaps due to the potential for a low temperature delta leading to a significant increase in measurement error. The most important parameter in this study is the air gap, illustrated by the significant decrease in efficiency for unalloyed steel from 69.3% at a 1mm air gap to 28.3% at a 9mm air gap at the same power output. Additionally, there is a noticeable trend of decreasing efficiency as the power output of the induction heating device is reduced. The margin of error was small throughout the series of experiments.

B. Results of Transient Experiments

The results of the transient heating experiments are shown in Table III and Table IV. The efficiency between the two workpieces stays nearly the same for the same air gaps and induction power. As in the steady-state experiments, it can be clearly seen that the efficiency also decreases sharply in the transient experiments with the air gap, e.g., for unalloyed steel the efficiency decreases from 47.41% at an air gap of 3 mm to 30.5% at 9 mm. Between the different widths of the material there is not much difference in efficiency, e.g. 33.89% for the wider workpiece compared to 34.75% for the narrower one, both at 3 mm air gap and 2.33 kW power and with stainless steel.

TABLE III: RESULTS TRANSIENT EXPERIMENTS LARGER WORKPIECE

Unit	Material; Width	Air gap mm	$P_{el\,AC}$ kW	η %
TS 3-1	Stainless 222mm	3	2.33	33.89
TS 3-2	Stainless 222mm	3	3.44	35.14
TS 6-1	Stainless 222mm	6	3.44	27.22
TS 6-2	Stainless 222mm	6	4.56	28.33
TS 9-1	Stainless 222mm	9	4.56	21.32
TS 9-2	Stainless 222mm	9	5.67	22.09
TU 3-1	Unalloyed 222mm	3	1.72	44.69
TU 3-2	Unalloyed 222mm	3	2.33	47.41
TU 6-1	Unalloyed 222mm	6	2.33	37.32
TU 6-2	Unalloyed 222mm	6	3.44	38.94
TU 9-1	Unalloyed 222mm	9	3.44	30.50
TU 9-2	Unalloyed 222mm	9	4.56	29.95

TABLE IV: RESULTS TRANSIENT EXPERIMENTS SMALLER WORKPIECE

Unit	Material; Width	Air gap mm	$P_{el\,AC}$ kW	η %
TS 3-3	Stainless 148mm	3	2.33	34.75
TS 3-4	Stainless 148mm	3	3.44	35.20
TS 6-3	Stainless 148mm	6	3.44	27.72
TS 6-4	Stainless 148mm	6	4.56	27.09
TS 9-3	Stainless 148mm	9	4.56	20.90
TS 9-4	Stainless 148mm	9	5.67	21.04
TU 3-3	Unalloyed 148mm	3	1.72	47.44
TU 3-4	Unalloyed 148mm	3	2.33	46.73
TU 6-3	Unalloyed 148mm	6	2.33	40.34
TU 6-4	Unalloyed 148mm	6	3.44	39.77
TU 9-3	Unalloyed 148mm	9	3.44	32.93
TU 9-4	Unalloyed 148mm	9	4.56	29.21

The most important results of this work can be seen in Fig. 7 and Fig. 8. Where the parameter field, between the efficiency, the power of the inductive heating device and the air gap, of the steady-state experiments are shown. This result is compared to the transient experiments in the same diagram.

The results show clearly that the transient results fit right with the trend of the validated parameter field, which can be seen as an upper limit for the efficiency. Therefore, the shown heating strategy of moving the inductor coil over the workpiece is proven to be efficient way to heat up sheet metal.

The experiment in which the temperature was held at the same level as the initial heat up can be seen in Fig 6. The shown diagram shows the workpiece made out of unalloyed steel with a width of 222 mm. As it is marked in the diagram the initial heat up was done with 2.3 kW, after this the power of the induction coil was reduced to 0.5 kW to hold the temperature at 140 ℃. Fig. 6 shows that the experiment was highly successful, with the temperature distribution across the nine thermocouples revealing only small deviations from the initial heat-up until the conclusion of the experiment at 200 s.

V. CONCLUSION

This paper presents two important findings. First, the method of providing a parameter field with steady-state measurements was proven to be highly accurate, with only a small error in the energy balances. As demonstrated in the efficiency calculation section of this paper, this measurement method allowed for the evaluation of induction heating efficiency without the need for numerical investigation. This work provides a foundation for future investigations. For instance, it is feasible to compare various geometries of induction coils or different materials of magnetic flux concentrators. The paper's second major finding is the successful implementation of the proposed method for heating sheet metal in small-scale experiments. The method exhibited no significant decrease in efficiency as the size of the workpiece increased. These findings can also be extended to the examination of larger workpieces. The parameter field of the steady-state experiments fits well with the transient experiments which reflect an industrial application, as demonstrated in Fig. 7 and Fig. 8. The insights gained from the transient experiments can be applied to other industrial applications. The temperature range used, up to 140 ℃, is similar to that used in paint curing and drying, where uniform temperature distribution is of major importance.

CONFLICT OF INTEREST

The authors declare no conflict of interest.

AUTHOR CONTRIBUTIONS

The presented idea was conceived by R. Gergely and C. Hochenauer; R. Gergely conducted the experiments and analysed the results; C. Hochenauer supervised the project; The paper was written by R. Gergely and C. Hochenauer; the final version was approved by both authors.

FUNDING

This work was financially supported by the Austrian Research Promotion Agency (FFG), Austria, "Prozess-

und Energieoptimierung mittels Induktion zum Aushärten der Korrosionsschutzschicht in der Automobilindustrie" (project 881147, eCall 35451221).

REFERENCES

[1] V. Rudnev, D. Loveless, and R. L. Cook, *Handbook of Induction Heating*, Imprimerie Noubelle Association Ouvriere, Paris, 2017.

[2] O. Lucia, P. Maussion, E. J. Dede, and J. M. Burdio, "Induction Heating Technology and Its Applications: Past Developments, Current Technology, and Future Challenges," *IEEE Trans. Ind. Electron.*, vol. 61, no. 5, pp. 2509–2520, 2014. doi:10.1109/TIE.2013.2281162

[3] G. Benkowsky, *Induktionserwärmung Härten, Glühen, Schmelzen, Löten, Schweissen Grundlagen und Praktische Anleitungen für Induktionserwärmungsverfahren, Insbesondere auf dem Gebiet der Hochfrequenzerwärmung*, 5th ed., Verl. Technik, Berlin, 1990.

[4] V. Rudnev and G. E. Totten, *ASM Handbook Volume 4C: Induction Heating and Heat Treatment*, ASM International, Ohio, 2014.

[5] R. E. Haimbaugh, *Practical Induction Heat Treating*, 2nd ed., ASM TECHNICAL BOOKS, Ohio, 2015.

[6] E. J. Davies, *Conduction and Induction Heating*, IET, Stevenage, 1990.

[7] (V. Rudnev). Systematic Analysis of Induction Coil Failures: Part 4: Coil Copper Electromagnetic edge effect. [Online]. Available: https://inducto.group/inductoheat-com/wp-content/uploads/sites/11/2019/05/Systematic-analysis-of-induction-coil-failures-Part-4.pdf

[8] T. Vibrans, "Induktive Erwärmung von Formplatinen für die Warmumformung," Dissertation an der Fakultät für Maschinenbau der Technischen Universität Chemnitz, Institut für Werkzeugmaschinen und Produktionsprozesse, Chemnitz, 2016.

[9] C. Liu, J. Han, R. Lu, J. Liu, "Explorative study on an online induction heating-based pilger rolling process for seamless treatment of high-frequency welded pipes," *Materials Today Communications*, vol. 35, #06068, 2023. doi: 10.1016/j.mtcomm.2023.106068

[10] J. Sun, W. Zhang, C. Shan, L. Wang, "Simulation and experimental research on local continuous induction heating of inner corrugated section," *International Communications in Heat and Mass Transfer*, vol. 147, #106980, 2023. doi: 10.1016/j.icheatmasstransfer.2023.106980

[11] M. Kranjc, A. Zupanic, D. Miklavcic, T. Jarm, "Numerical analysis and thermographic investigation of induction heating", *International Journal of Heat and Mass Transfer*, vol. 53, pp. 3585–3591, 2010. doi: 10.1016/j.ijheatmasstransfer.2010.04.030

[12] H.-T. Bui, S.-J. Hwang, "Modeling a working coil coupled with magnetic flux concentrators for barrel induction heating in an injection molding machine", *International Journal of Heat and Mass Transfer*, vol. 86, pp. 16–30, 2015. doi: 10.1016/j.ijheatmasstransfer.2015.02.057

[13] J. Sun, S. Li, C. Qiu, Y. Peng, "Numerical and experimental investigation of induction heating process of heavy cylinder", *Applied Thermal Engineering*, vol. 134, pp. 341–352, 2018. doi: 10.1016/j.applthermaleng.2018.01.101

[14] R. Gergely, C. Hochenauer, "Heating Strategies for Efficient Combined Inductive and Convective Heating of Profiles", *Energies*, vol.16, #5895, 2023. doi:10.3390/en16165895

[15] M. Patil, R. Kumar Choubey, P. Kumar Jain, "Influence of coil shapes on temperature distribution in induction heating process", *Materials Today: Proceedings*, vol.72, pp. 3029–3035, 2023. doi: 10.1016/j.matpr.2022.08.376

[16] W. Jin, C. Xing, Y. Lu, S. Baoshou, D. Li, "A novel method improving the temperature uniformity of hot-plate under induction heating", *Journal of Mechanical Engineering Science*, vol.235(I), pp. 190–201, 2021. doi:10.1177/0954406220936307

[17] X. Fu, M. Ma, S. Wang, C. Teng, W. Liang, "Heat generation and transfer simulation of a high temperature heat pipe under induction heating based on a coupled model", *Applied Thermal Engineering*, vol.232, #121025, 2023. doi: 10.1016/j.applthermaleng.2023.121025

[18] Y. Wang, X. Hu, M. Jiang, J. Wang, M. Wei, L. Zhang, "Temperature field characterization and optimization of temperature field distribution in pipe lining process based on electromagnetic induction heating system", *Case Studies in Thermal Engineering*, vol.28, #101609, 2021. doi: 10.1016/j.csite.2021.101609

[19] H. Wen, X. Zhang, H. Ye, Y. Han, "Research on the mechanism of magnetic flux concentrator in the gap-to-gap induction heating of wind power gear", *International Journal of Thermal Sciences*, vol.168, #107055, 2021. doi: 10.1016/j.ijthermalsci.2021.107055

[20] P. Yang, Z. Hong, Z. Jin, "Heat behavior and axial temperature distribution of a Ti-6Al-4V alloy in a superconducting induction heater with a controllable magnet structure", *Applied Thermal Engineering*, vol.236, #121516, 2024. doi: 10.1016/j.applthermaleng.2023.121516

[21] A. Zhang, Y. Zuo, M. Zhang, H. Zhou, "Numerical study on thermal performance and thermal stress of molten salt receiver tube based on induction heating", *Applied Thermal Engineering*, vol.235, #121353, 2023. doi: 10.1016/j.applthermaleng.2023.121353

[22] VDI Gesellschaft, *VDI-Wärmeatlas*, 11. Auflage, Springer Berlin Heidelberg, Berlin, Heidelberg, 2013.

Raphael Gergely holds a bachelor's and master's degree in mechanical engineering from Graz University of Technology, earned in 2018 and 2021, respectively. Currently a scientific project member at the Institute of Thermal Engineering at Graz University of technology, he boasts a publication in a Scopus-indexed journal. His research focuses on induction and convective heating, CFD, and improving heating system efficiency.

Christoph Hochenauer graduated from Graz University of Technology with a master's degree in mechanical engineering in 2003. He completed his PhD in 2005 at Graz University of technology. He has held various roles, including CFD Engineer at Austrian Energy and Environment (2005-2007) and full Professor at Upper Austrian University of Applied Sciences (2007-2012). Since 2012, he has been a full Professor and Head of the Institute of Thermal Engineering at Graz University of Technology. His research interests include combustion systems, numerical simulation of chemically reacting flows, heat transfer in furnaces and boilers, flue gas and syngas cleaning, fluid-solid interactions and solid oxide fuel cells (SOFCs). He has led multiple national and industry-funded projects, authored and co-authored over 200 contributions to journals and conference proceedings, and serves as a reviewer for established journals.